ACS OMEGA

http://pubs.acs.org/journal/acsodf

Article

Study on the Staged and Direct Fast Pyrolysis Behavior of Waste Pine Sawdust Using High Heating Rate TG-FTIR and Py-GC/MS

Jinhong Zhang,* Daniel T. Sekyere, Noah Niwamanya, Yansheng Huang, Andrew Barigye, and Yuanyu Tian*

Cite This: *ACS Omega* 2022, 7, 4245−4256

Read Online

ACCESS | Metrics & More | Article Recommendations | Supporting Information

ABSTRACT: To understand the fast pyrolysis kinetics and product evolution of waste pine sawdust, high heating rate thermogravimetry-Fourier transform infrared (TG-FTIR) was used to obtain the kinetic parameters and the chemical groups formed during the pyrolysis process, while pyrolysis-gas chromatography/mass spectrometry (Py-GC/MS) was used to investigate the detailed compositions of products under the staged (seven stages from 300 to 600 °C) and direct fast pyrolysis process. Spectral bands were identified for acids, alcohols, aldehydes, aromatics, esters, ethers, hydrocarbons, ketones, phenols, and sugars. Research found that the apparent activation energy for fast pyrolysis is much higher than that of slow pyrolysis. The evolution of CO_2 is the major deoxygenation route. Cracking mainly occurred at the 450 °C stage with phenols, ketones, aldehydes, and sugars as the main products. The product distributions for different stages are significantly different; the selectivity of aldehydes decreased, while phenols showed an upward trend with an increase in pyrolysis temperature. Ketones and sugars reached their peak values at 450 °C. The changes in the molecular composition of each stage helped to understand the pyrolysis process. Compared with the staged pyrolysis, the direct pyrolysis process had higher selectivity of acids, aldehydes, esters, and sugars and lower selectivity of phenols, ketones, and alcohols.

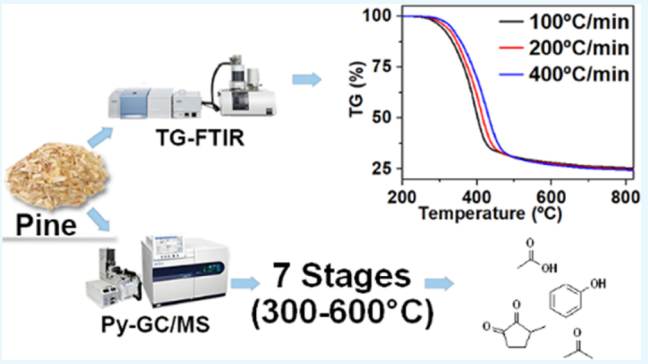

1. INTRODUCTION

The energy demand is increasing and the unsustainable nature of fossil fuel has sprung up research into alternative energy and fuels with biomass energy being one of the frontiers because it is renewable, economical, and carbon neutral. Several studies have been done in the quest to upgrade bio-oil to reach the fuel standard but its challenges of high acidity, chemical instability, and low heating value linger on.[1−3] Although, the general classes of products evolved from biomass pyrolysis are known, in-depth compositional analysis of the compounds evolved has not been studied extensively, making it rather difficult to address these drawbacks. This is because there are hundreds of compounds in bio-oil, and it is challenging to separate the complex components.[4] That notwithstanding, several studies have been done to help remedy the drawbacks related to bio-oil. Some of the studies include copyrolysis and catalytic copyrolysis of biomass with hydrogen-rich materials and copyrolysis of biomass and amino acids.[5−10]

Py-GC/MS is a powerful tool to identify the compounds evolved from the pyrolysis process and has been widely used to investigate the fast pyrolysis behavior of biomass. The process of direct pyrolysis has been extensively researched.[1,11−14] Some researchers investigated two-staged pyrolysis; the first stage is usually done between the temperatures of 200 and 360 °C and the second stage is done at elevated temperatures of over 500 °C.[1,15,16] Cai et al.[1] carried out two-staged pyrolysis of biomass using Py-GC/MS, and found that the pyrolysis products from the first stage were enriched with compounds like organic acids, alcohols, and aldehydes with a high portion of the second stage pyrolysis products being phenols. Zhang et al.[4,16,17] studied the effect of residence time and step temperatures on the product distribution of biomass pyrolysis in two-step pyrolysis, and found that the retention time had little effect on the contents of anhydrosugars and their derivatives. Also, the contents of aromatics increased at first and later decreased with the increase in pyrolysis temperature. Tubetskaya et al.[18] identified that the inorganic contents such as metals found in biomass can act as catalysts for the pyrolysis process, thus influencing the product distribution. It can be inferred that there is an apparent increase in the inorganic content after each step of staged pyrolysis, implying that the

Received: October 21, 2021
Accepted: January 12, 2022
Published: January 25, 2022

https://doi.org/10.1021/acsomega.1c05907
ACS Omega 2022, 7, 4245−4256

subsequent processes can yield high-quality and stable bio-oils. Previous research, on the other hand, focused mostly on direct or two-stage pyrolysis.

Thermogravimetry (TG) is a useful technique for analyzing solid−gas reactions. Its time-dependent weight change curves are the basis for characterizing the devolatilization processes, quantification of release rates, and determination of kinetic parameters. With its fastness and sensitivity, the major functional groups of the volatile species and temperature range of products evolution of the pyrolysis process can be detected accurately by TG coupled with an FTIR detector. There are a lot of studies that used TG-FTIR to study the pyrolysis kinetics of biomass. However, most of them used low heating rates (slow pyrolysis), usually lower than 50 °C/min. Thus, more work needs to be done using the high heating rate TG-FTIR to study the fast pyrolysis behavior of biomass. Moreover, several studies using different biomasses have been done on the low heating rate kinetics,[19−22] with a few of these studies being on the high heating rates kinetics.[23−25] Thus, the kinetics of the high heating rate and the low heating rate cannot be compared based on these previous studies, hence the need for further studies.

To mimic the industrial condition of fast pyrolysis, the high heating rate TG-FTIR was used to study the fast pyrolysis kinetics of waste pine sawdust and detect the chemical groups formed during the pyrolysis process. Moreover, the low heating rate kinetics was also studied to differentiate the fast pyrolysis kinetics from the slow pyrolysis kinetics. This work aims to provide in-depth identification of the compounds that evolved during the pyrolysis of biomass as well as provide possible reaction pathways. Seven-stage pyrolysis from 300 to 600 °C was carried out by Py-GC/MS. The effect of each stage on the products evolved in contrast to that of the direct pyrolysis process was investigated.

2. MATERIALS AND METHODS

2.1. Materials. In this work, waste pine sawdust with a size between 80 and 200 mesh (0.075−0.18 mm) was used. It was dried at 105 °C for 12 h. A high-speed crusher (220 V, 50 Hz, 1800 W, 28 000 r/min, and mesh size of 30−300) was used to mill the pine chips. Table 1 shows the main properties of the pine sawdust. Proximate analysis of the pine sawdust on a dry basis was performed according to the Chinese National Standard (GB/T 28731-2012). The ultimate analysis was measured by an Elementar Analysensyteme Gmbh (Vario MACRO cube, Germany). The fixed carbon content and the oxygen content were calculated by the difference. The values obtained for the proximate and ultimate analyses are close to literature values, indicating the suitability of pine for pyrolysis.[12,16,26−28]

Table 1. Proximate Analysis and Ultimate Analysis of Raw Materials

proximate analysis (wt %)[a]			ultimate analysis (wt %)				
volatiles	fixed carbon	ash	C	H	O[b]	S	N
81.89	15.84	2.27	49.56	5.63	44.74	0.02	0.05

[a]Dry basis. [b]Calculated by the difference.

2.2. TG-FTIR Analysis. Thermogravimetric analysis (TG) is usually employed in studying the thermal pyrolysis behavior of biomass.[11,12,14,26,29−32] Herein, TG analysis of pine was performed at high heating rates of 100, 200, and 400 °C/min using a thermogravimetric analyzer (STA 449F3 NETZSCH Company, Germany) with a high-speed heating furnace (NETZSCH Company, Germany). The description of the high-speed heating furnace can be found elsewhere.[25] Different heating rates were employed to help comprehend the pyrolysis dynamics and estimate the apparent activation energy of the sample. The TG equipment was coupled to a Fourier transform infrared spectrometer (FTIR TENSOR II, BRUKER Company) using a 1 m long Teflon tube transfer line with an internal diameter of 2 mm for online analysis of the gaseous products released during pyrolysis. To mitigate the possibility of gas condensation, the transfer line was heated and maintained at 200 °C. The spectra were collected at a resolution of 4 cm^{-1} over the range of 4000−500 cm^{-1}, and the spectrum scan frequency was 32 times per minute. Slow pyrolysis was done using a simultaneous DTA-TG apparatus (DTG-60H, Shimadzu) at 10, 20, and 40 °C/min. Approximately, 5 mg of the sample was used for all TG experiments. A flow rate of 100 mL/min was used in all TG experiments with nitrogen as a carrier gas for fast pyrolysis and argon as a carrier gas for slow pyrolysis.

2.3. Kinetic Analysis. The kinetics of the decomposition of biomass is a complex process but is usually modeled to follow this general reaction pathway.[29,32,33]

$$\text{biomass} \xrightarrow{k} \text{volatiles} + \text{char} \tag{1}$$

where k is defined as the rate constant of the reaction with its temperature dependence expressed by the Arrhenius equation.

$$k = A e^{-E_a/RT} \tag{2}$$

where E_a is the apparent activation energy (kJ/mol), T is the absolute temperature (K), R is the universal gas constant 8.314 J/mol·K, and A is the pre-exponential factor (s^{-1}).

The rate of conversion of the biomass to volatiles is given by the expression

$$\frac{d\alpha}{dt} = k(T) f(\alpha) \tag{3}$$

where α is the conversion ratio of pine at time t(s), k is the rate constant, and $f(\alpha)$ is the reaction model.

$$\alpha = \frac{m_o - m_t}{m_o - m_f} \tag{4}$$

The reaction model is given by eq 5

$$f(\alpha) = (1 - \alpha)^n \tag{5}$$

where m_t is the weight at any time t, m_o is the initial weight at the start of that stage, and m_f is the final weight at the end of that stage.

Model-free methods like Freidman, Flynn−Wall and Ozawa (FWO), and Kissinger−Akahira−Sonuse (KAS) are the most frequently used approximations in estimating the reaction kinetics.[21,23] The functions $f(\alpha)$ and $g(\alpha)$ are $(1 - \alpha)$ and $(-\ln(1 - \alpha))$, respectively, expressed using reaction order models for a first-order reaction.[11,21,26]

Freidman's approximation is given by the studies[14,19]

$$\ln\left(\beta \frac{d\alpha}{dT}\right) = \ln[A f(\alpha)] - \frac{E_a}{RT} \tag{6}$$

The apparent activation energy can be obtained from a plot of $\ln(\beta\, d\alpha/dT)$ against $1/T$ for a given value of conversion α,

https://doi.org/10.1021/acsomega.1c05907
ACS Omega 2022, 7, 4245−4256

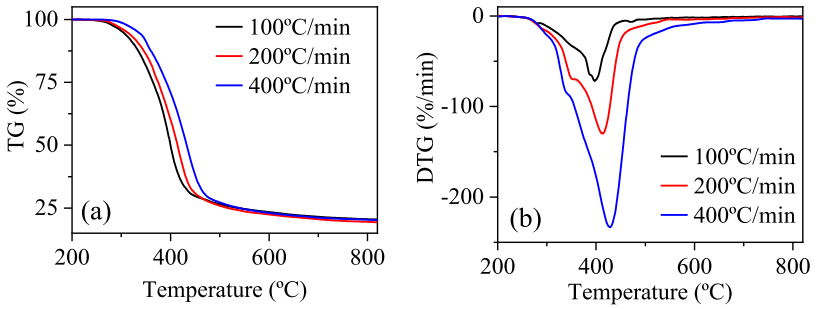

Figure 1. TG and DTG curves under high heating rates. (a) TG and (b) DTG.

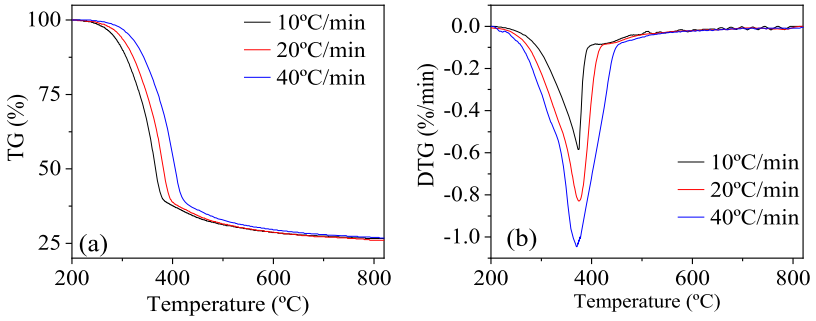

Figure 2. TG and DTG curves under low heating rates. (a) TG and (b) DTG.

where the slope is equal to E_a/R. The apparent pre-exponential factor can be found from the expression $A = (\exp^C)/(1 - \alpha)$, where $C = \ln[Af(\alpha)]$.

Kissinger−Akahira−Sonuse (KAS) approximation is expressed as[11,25]

$$\ln\left(\frac{\beta}{T^2}\right) = \ln\left(\frac{AR}{E_a g(\alpha)}\right) - \frac{E_a}{RT} \quad (7)$$

A plot of $\ln(\beta/T^2)$ vs $1/T$ is made and the apparent activation energy E_a, is calculated from the slope $m = -E_a/R$. The pre-exponential factor is then calculated from the expression $A = (E_a[-\ln(1 - \alpha)]\exp^C)/R$

Flynn−Wall−Ozawa (FWO) approximation is also given by[11,25]

$$\ln(\beta) = \ln[\frac{AE_a}{Rg(\alpha)}] - 5.335 - 1.052\frac{E_a}{RT} \quad (8)$$

Apparent activation energy E_a, is estimated as $E_a = (-mR)/1.052$, where m is the slope. The pre-exponential factor A is estimated as $A = (R[-\ln(1 - \alpha)]\ \exp^{C + 5.335})/E_a$.

2.4. Py-GC/MS Analysis. The pyrolysis-gas chromatography/mass spectrometry (Py-GC/MS) technique was exploited in this study to separate and identify the pyrolysis products at different temperatures. The details of the equipment used are the same as described by Wang et al.[25] The experiment was carried out in two different ways, staged pyrolysis and direct pyrolysis. For the staged pyrolysis, about 1 mg of the sample was sandwiched between quartz wool inside a quartz tube and placed in a pyroprobe made of a platinum wire. The pyroprobe was then heated from room temperature to the set temperature, starting from the initial stage temperature of 300 °C with an increase of 50 °C for each stage to the final stage temperature of 600 °C. The heating rate was set as 10 °C/ms to reach the desired temperature in milliseconds; thus, the influence of the heating process can be ignored. The heating time of samples during pyrolysis was 10 s per run. For the direct pyrolysis, about 0.2 mg of the sample was used for each run at temperatures of 500, 550, and 600 °C. The chromatographic separation of volatile products was performed using an Agilent DB-5 MS capillary column (60 m × 0.25 mm, 0.25 μm film thickness). Helium was used as a carrier gas at a constant rate of 40 mL/min. The temperature conditions used by the chromatographic column for separation are as follows: it was held at an initial temperature of 35 °C for 10 min, and the temperature was then increased to 200 °C at a rate of 3 °C/min. The temperature was further increased to 280 °C at a rate of 4 °C/min and finally increased to 300 °C at a rate of 10 °C/min. The mass spectrometer was operated in an EI mode at 70 eV, and the mass spectra were obtained from m/z 20 to 500. The chromatographic peaks were identified according to the NIST MS library.

3. RESULTS AND DISCUSSION

3.1. Thermogravimetric Analysis. The TG/DTG curves of pine at high and low heating rates are shown in Figures 1,2, respectively. High heating rates of 100, 200, and 400 °C/min were used to study the fast pyrolysis kinetics in contrast to the low heating rates usually lower than 50 °C/min, which are generally used.[11,12,14,26,31,32,34,35] The use of a high heating rate was to simulate the industrial setting and to provide alternative kinetic data for biomass pyrolysis different from that of low heating rates kinetics, which is readily available. The sample was well dried before the experiment, thus eliminating the dehydration stage as observed by other researchers.[11,12,14,36] Four runs of experiments were conducted. The average ash content for 100, 200, and 400 °C/min were 22.07 ± 0.27, 21.62 ± 0.27, and 20.50 ± 0.36, respectively (see Figure S1 for the thermograms of the four runs).

The active pyrolysis (main weight loss) stage is composed of the fast decomposition of hemicellulose and cellulose and the slow decomposition of lignin. The passive pyrolysis stage is

https://doi.org/10.1021/acsomega.1c05907
ACS Omega 2022, 7, 4245−4256

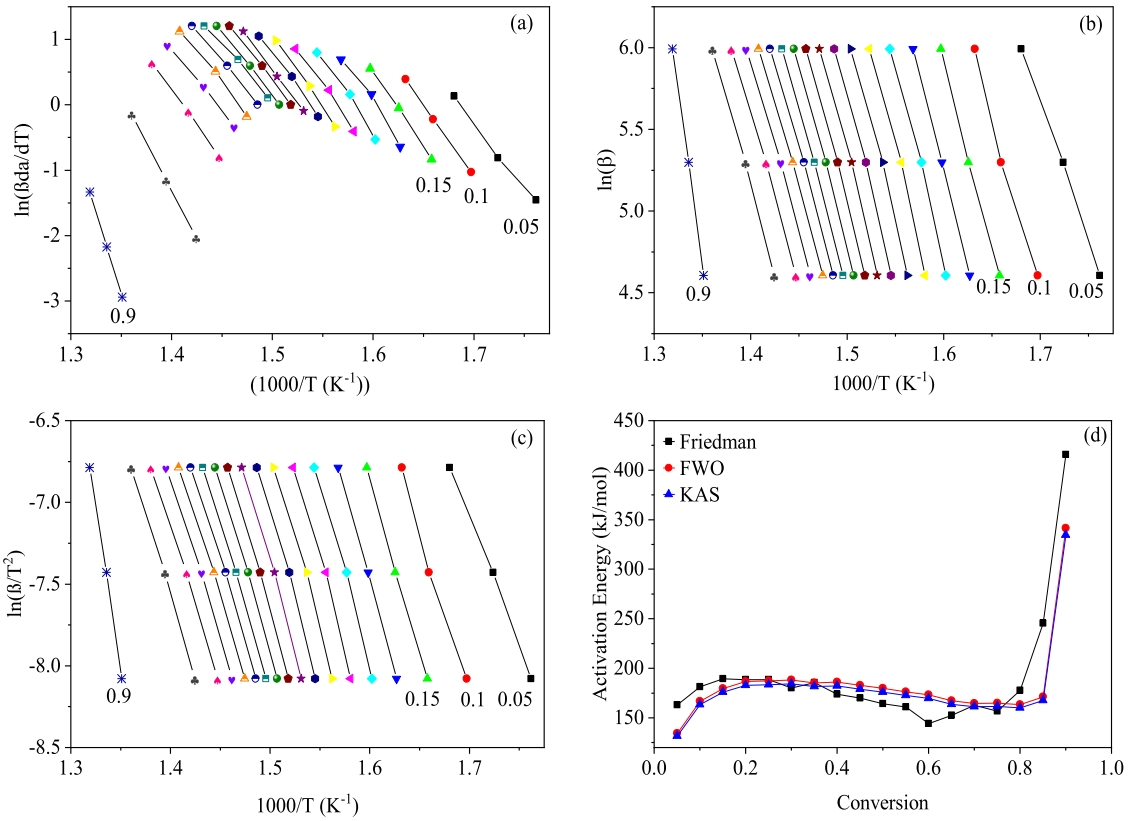

Figure 3. Plots of the model-free methods for high heating rates. (a) Friedman, (b) FWO, (c) KAS, and (d) plot of activation energy vs conversion.

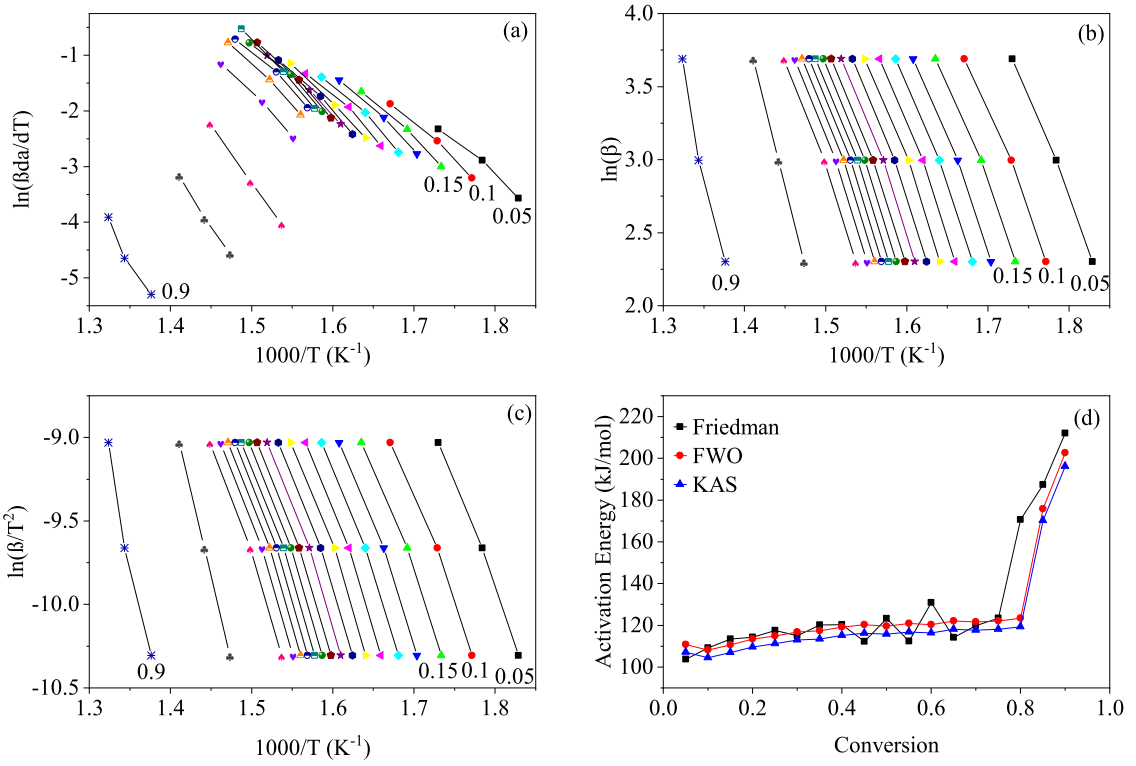

Figure 4. Plots of the model-free methods for low heating rates. (a) Friedman, (b) FWO, (c) KAS, and (d) plot of activation energy vs conversion.

associated with the further cracking of pine due to lignin. The onset of the decomposition of the components of biomass is not fixed as different researchers report noticeably different temperatures based on their studies. However, it has been proven that cellulose and hemicellulose decompose rapidly over a short temperature range, while lignin decomposes slowly over a wider temperature range until the final temperature of the experiment.[1,26,35,37−41] Active pyrolysis occurred between

https://doi.org/10.1021/acsomega.1c05907
ACS Omega 2022, 7, 4245−4256

250 and 490 °C with a sharp decrease in the pine weight corresponding to about 71.6% decomposition of the total weight. Passive pyrolysis occurred after 490 °C to the final temperature of the experiment at 820 °C, corresponding to a loss of 7.1% of the total weight, thus obtaining a total weight loss of 78.7%. The mass loss of pine increased slightly as the heating rate increased, which is similar to the observation made by Li et al.[38] For slow pyrolysis (Figure 2), a total weight loss of 73.4% was observed, with 62.4% occurring during the active pyrolysis stage (240−400 °C) and 11.0% occurring during the passive pyrolysis stage. The char yield for slow pyrolysis was higher than that of fast pyrolysis. This could be attributed to the relatively long residence time of the slow pyrolysis process, which led to the easy formation of an anhydro-cellulose phase with the loss of only water making it prone to char formation[15] and the enhancement of secondary cracking in the reactor, which further increased the char yield.[25]

Pine like any other lignocellulosic biomass has three main components, hemicellulose (20.3−24%), cellulose (45.6−46.9%), and lignin (26.8−27.3%).[3,41] Two peaks were visible on the DTG curves; the first shoulder peak was due to the decomposition of hemicellulose and the second peak was due to the decomposition of cellulose.[4] The appearance of the maximum peaks of devolatilization of the components of biomass at different temperatures suggests that the components decompose sequentially with a little overlap. The maximum decomposition temperature of the various components shifted to higher temperatures as the heating rate increased due to the formation of thermal hysteresis, which resulted from heat transfer limitation.[25,26,31]

3.2. Kinetic Analysis. The apparent activation energy, E_a, and the pre-exponential factor, A, for pine were calculated from the model-free isoconversional methods Friedman, FWO, and KAS using the thermogravimetric curves from the three different heating rates. Figures 3 and 4 show the plots of the models used and a plot of E_a against conversion for high and low heating rates, respectively. The conversion rate of 0.05−0.9 at an interval of 0.05 was used to estimate the kinetic parameters. The curve for FWO and KAS almost overlapped with very little variations, which are due to the different approximations used to estimate the temperature integral in these methods. The Friedman method, however, differed from the trend of FWO and KAS, which can be attributed to its drawback of being a differential method applied to integral data, thus sometimes yielding scattered E_a values.[26]

The two pyrolysis processes followed a similar E_a trend between the conversions of 0.05 and 0.3, as shown in Figures 3d and 4d. After 0.3, the trend decreased for a high heating rate because the active cellulose formed had lower molecular weight and required lower energy for decomposition. On the contrary, the trend continued to increase for a low heating rate after 0.3 because of the relatively long residence time of the volatiles. This caused the volatiles evolved to cover the surface of the sample to form carbonaceous char, which acts as a physical barrier insulating the heat from reaching the surface below and preventing the diffusion of combustible gases. Thus, for low heating rates, more energy is required to activate the reaction as conversion increases. However, both processes followed the same trend after 0.75 with a sharp increase in E_a values due to the degradation of lignin and char. High heating rate kinetics, showed an increase in E_a from 0.05 to 0.30 due to the initial breaking of bonds and decreased slightly until 0.08.[11,12,14,25]

For high heating rates, the average E_a was 189.03, 183.35, and 179.64 kJ/mol for Friedman, FWO, and KAS with corresponding A values of 6.50×10^{27}, 1.44×10^{27}, and 6.59×10^{20} s^{-1}, respectively.

A summary of the kinetic parameters is provided in Table 2. The kinetic parameters at different conversions for both high and low heating rates are shown in Tables S1 and S2 respectively. The average E_a values obtained from the slow pyrolysis using Friedman, FWO, and KAS methods are 128.9, 125.6, and 121.5 kJ/mol, respectively. The average values of E_a obtained for fast pyrolysis were higher than those of slow pyrolysis. The E_a values for the slow pyrolysis were similar to those observed in other works.[12,26] For both slow and fast pyrolysis, high correlation values were obtained, indicating that the models used and the first-order approximation duly fitted and described the pyrolysis process. Biomass has poor thermal conductivity, thus the transfer of heat in pine also contributes to the reaction at higher heating rates, resulting in higher E_a values, as observed by Wang et al.[25]

Table 2. Summary of the Kinetic Parameters for High and Low Heating Rates for Different Kinetic Models

kinetic model	ramp rate	E_a (kJ/mol)	A (min^{-1})	R^2
Friedman	LHR	128.93	5.95×10^{12}	0.9912
	HHR	189.03	6.50×10^{27}	0.9963
FWO	LHR	125.61	2.38×10^{16}	0.9928
	HHR	183.36	1.44×10^{27}	0.9969
KAS	LHR	121.48	1.34×10^{10}	0.9921
	HHR	179.64	6.59×10^{20}	0.9967

3.3. FTIR Spectra Analysis. FTIR is a technique employed to study the nature of evolved gases during pyrolysis.[35,42−44] Usually, the spectra obtained at the maximum decomposition of the biomass based on the TG curves are analyzed.[1,7,11,12,35] The three-dimensional (3D)-FTIR spectrum of the pyrolysis process can be seen in Figure 5. The evolution profile of the evolved products is shown in Figure 6, while Figure 7 shows the spectra at various stages (300−600 °C).

The spectral range detected at 3700−3500 cm^{-1} is related to the stretching vibrations of the O−H group, demonstrative of phenols, water, or alcohols. The H_2O released was mainly due to the presence of bound water and the cracking reaction of the oxygen functional groups in the pyrolysis process as the temperature increased since there was a negligible amount of free water. Thus, the release of H_2O is an important deoxygenation route for the pyrolysis of biomass. Dehydration at adjacent carbon positions forms C−C and C−O organics, while dehydration at nonadjacent carbon positions mainly produces sugars (Figure 8).[1,11]

The absorbance peak 2359 cm^{-1} (range 2400−2250 cm^{-1}) was the most prominent in all of the spectra, indicating the release of CO_2. A relatively weaker peak of CO_2 that appeared between 600 and 750 cm^{-1} was attributed to the secondary degradation of C═O and C−O compounds.[11] As shown in Figure 6a, the emission of CO_2 first increased with the increase in temperature, then decreased dramatically after 330 °C till the temperature reached 390 °C, and finally went up again before decreasing gradually after 420 °C. The band at 3100−2850 cm^{-1} indicates the presence of aliphatic hydrocarbons in the pyrolysis product, while the peak at 3016 cm^{-1} in this band corresponds to the presence of CH_4 in the pyrolysis products.[6] The intensity of CH_4 peaked at 350 °C, as can be seen from

https://doi.org/10.1021/acsomega.1c05907
ACS Omega 2022, 7, 4245−4256

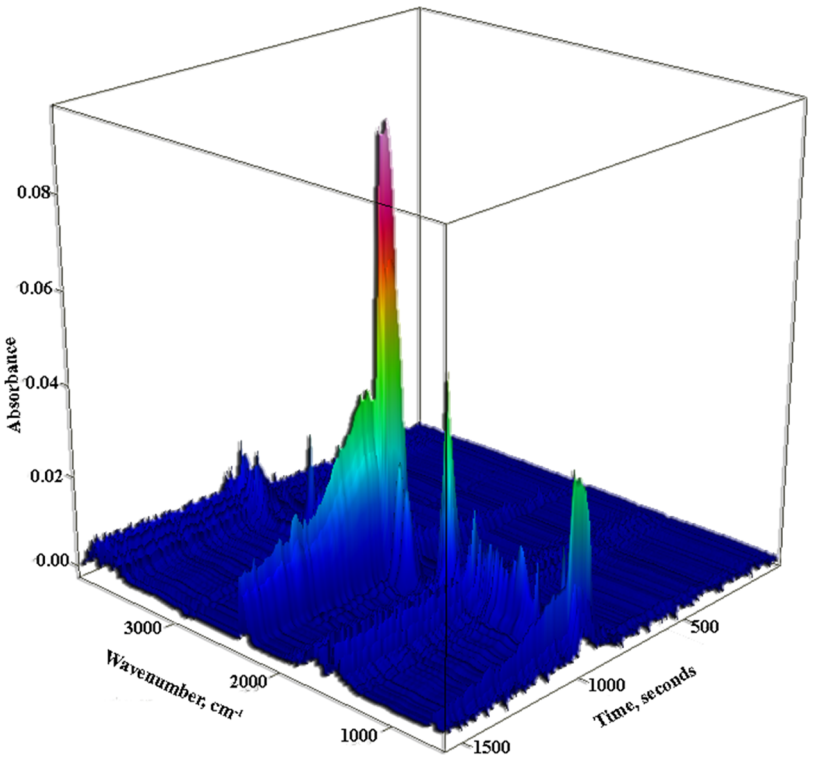

Figure 5. 3D-FTIR spectrum of pine pyrolysis.

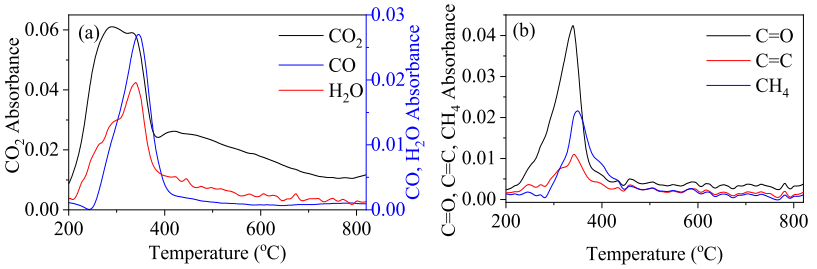

Figure 6. FTIR analysis results of the evolution profiles of some products during pine pyrolysis. (a) CO_2, CO, and H_2O and (b) C═O, C═C, and CH_4.

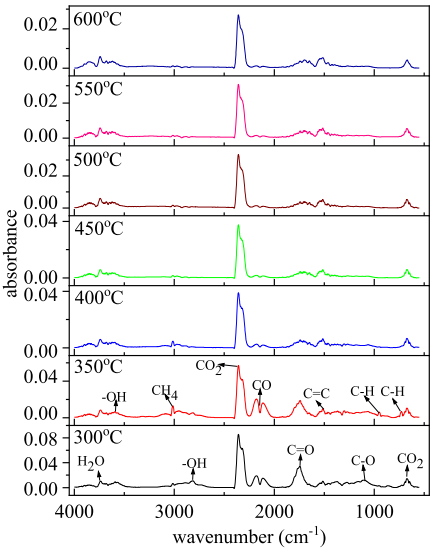

Figure 7. FTIR spectra at various stage temperatures.

Figure 6b, signifying a high production of CH_4 at the 350 °C stage than at any other stage. The formation of CH_4 can be attributed to the fragmentation of side chains and demethylation of methoxyl groups.[30]

The −CH bending vibrational peak at 950 cm^{-1} in the spectral range of 975−780 cm^{-1} at the stages of 300−400 °C identified the characteristic of aldehydes. The intensity of this peak was higher at 350 °C those at 300 and 400 °C, which is consistent with the Py-GC/MS results, as 350 °C had the highest yield of aldehydes. The −C═C− skeletal vibrational spectral range identified between 1650 and 1430 cm^{-1} is significant for the benzene ring, which is present in both phenols and aromatics.[35] Moreover, the absorbance wave of 730−620 cm^{-1} with a peak of 671 cm^{-1} can also be related to the C−H bond evident in aromatics.[14]

The absorbance waves between 2250 and 2040 cm^{-1} were related to the CO release with peaks at 2180 and 2110 cm^{-1}. The intensity of CO absorbance peaked at 350 °C and reduced sharply to 420 °C before reducing steadily with a further increase in temperature. This could imply that, at 350 °C, the carbonyls (C−O−C) and carboxyls (C═O) formed are thermally unstable and as such degrade easily, leading to a

https://doi.org/10.1021/acsomega.1c05907
ACS Omega 2022, 7, 4245−4256

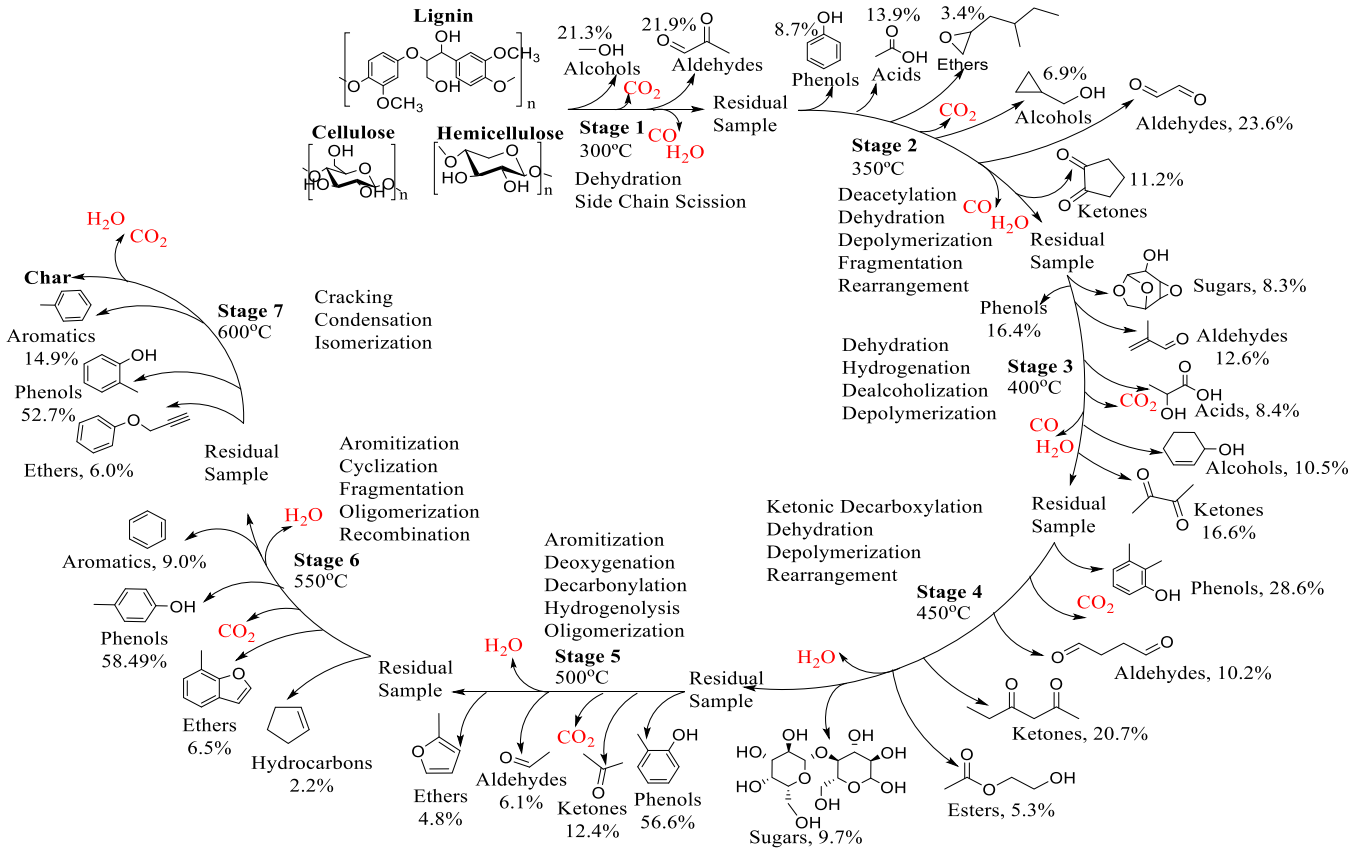

Figure 8. Summary of the main reactions and compound groups evolved at every stage.

high concentration of CO (Figure 6).[38] The characteristic bands of the C−O stretching vibration at 1250−1000 cm^{-1} and the C═O stretching at 1755−1650 cm^{-1} indicate the formation of carbonyls like aldehydes, ketones, esters, organic acids, or alcohols. However, the aliphatic hydroxyl group appeared in the bandwidth of 3000−2800 cm^{-1}. The bandwidths of O−H at 3700−3500 cm^{-1} and C−O at 1210−1015 cm^{-1} represent the presence of phenols and aliphatic ethers, respectively.[1] The C−O stretching vibration absorbance wave appeared from 1250−1000 cm^{-1} and the −C−H bending vibration absorbance wave between 750 and 650 cm^{-1} indicates the existence of alcohols.[12] From Figure 6 it can be seen that the C═O, C═C, and H_2O evolution curves all peaked around 340 °C, and steeped down to 420 °C before decreasing steadily. Table 3 gives a summary of the FTIR bands identified and the related chemical bonds and compounds.

3.4. Py-GC/MS Analysis. To know the fast pyrolysis behavior of pine, the staged and direct pyrolysis process was investigated by Py-GC/MS. The total ion count (TIC) of the gases that evolved was compared to the NIST library to determine the compounds. The compounds were grouped under acids (±0.30), alcohols (±1.10), aldehydes (±0.90), aromatics (±0.51), CO_2 (±0.73), esters (±0.20), ethers (±0.21), hydrocarbons (HC, ±0.11), ketones (±0.37), N-containing (±0.29), phenols (±0.53), sugars (±0.23), and others (±0.24).[11,28]

3.4.1. Staged Fast Pyrolysis. Figure 9a shows the percentage composition of the pyrolysis products at each stage. The first stage (300 °C) generated alcohols, aldehydes, and gases, which were mainly CO_2. A small amount of CO and

Table 3. Summary of the FTIR Band and Related Chemical Bonds and Compounds

wavenumber (cm^{-1})	chemical bond or group
4000−3400, 2000−1250	O−H stretching vibration; water
3100−3010, 3000−2850, 950	aliphatic hydrocarbons
1650−1430	−C═C− skeletal vibration; aromatics and phenols
975−780	−C−H bending vibration; aldehydes
750−650	−C−H bending vibration; alcohols
2250−2040	CO
1250−1000	C−O stretching vibration; alcohols
2400−2250, 750−600	CO_2
1755−1540	C═O stretching vibration; aldehydes; ketones
1740−1650	C═O stretching vibration; acids
3335−2500	O−H stretching vibration; acids
3700−3500	O−H stretching vibration; phenols
1210−1015	C−O stretching vibration; aliphatic ethers

CH_2O could be identified by the FTIR spectra, but could not be distinctively separated by a column. H_2O and CH_4 also could be identified from the FTIR spectra, but due to the low m/z values, they could not be detected by an MS detector. Alcohols were predominantly produced in the first stage of the pyrolysis, and their content decreased with the increase in temperature.[1] Thus, the O−H stretching vibration in the first-stage FTIR spectra can be ascribed to the presence of alcohols and water. The formation of methyl alcohol and methyl glyoxal (MG) suggests that the main reactions at the first stage were dehydration and breaking of the side chains of cellulose and hemicellulose components of the biomass. MG is known to be

https://doi.org/10.1021/acsomega.1c05907
ACS Omega 2022, 7, 4245−4256

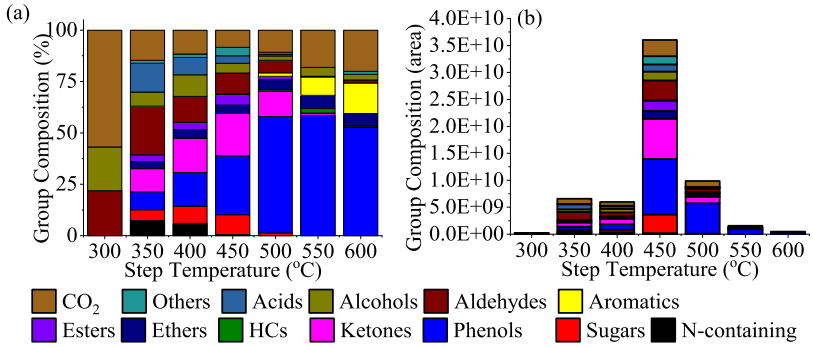

Figure 9. Product distribution of staged pyrolysis by (a) percentage and (b) peak area.

formed from the decomposition of sugars such as levoglucosan (LG) with byproducts like formic acid and glycolaldehyde. However, the absence of these products in the first stage suggests that MG present was formed via a different route. Nonetheless, LG and 1-hydroxy-2-propanone are formed from the competitive depolymerization of active cellulose.[45] LG was not identified in the stage pyrolysis products. On the other hand, 1-hydroxy-2-propanone was formed at the stages of 350, 400, 450, and 500, accounting for 4.96, 7.40, 7.38, and 1.63%, respectively. This implies that the formation of 1-hydroxy-2-propanone is the preferred route for the depolymerization of active cellulose. Products from lignin pyrolysis were not detected at the first stage, which implies that lignin only started decomposing at the second stage (350 °C). Subsequent stages produced more cyclic alcohols such as cyclopropyl carbinol, furanmethanol, 2-cyclohexen-1-ol, etc. This could be attributed to the fact that dehydration reactions occurred in the early stages, leading to the formation of a more cross-linked structure, thereby increasing the formation of cyclic compounds upon further pyrolysis at later stages.[46] Cyclic alcohols formed the majority of the alcohols produced and they were generated by the hydrogenation, dealcoholization, and subsequent hydrogenation of guaiacols.[47]

Acids were generated at 350 °C, and their content gradually decreased with the temperature increase. After 500 °C, no acids were detected. Deacetylation of depolymerized fragments of hemicellulose produced acetic acid, which was the main acidic product generated in the stages of 350, 400, and 450 °C, accounting for 99.72, 96.54, and 73.92% of the yield of the acid, respectively. At 500 °C, the acids present can be associated with secondary reactions like fragmentation of end chains and recombination of volatiles. Carboxylic acids underwent unimolecular decomposition, esterification reactions, redox reactions, and also acted as catalysts for the dehydration of other products.[48] At 350 °C, all groups of compounds were present except hydrocarbons and aromatics, which started appearing at 450 °C. Sugars and esters were detected at the stages of 350−500 °C and peaked at 450 °C. Depolymerization of cellulose leads to the formation of anhydrosugars, with levoglucosan being the main anhydrosugar formed. However, in our work, levoglucosan was not identified but rather served as an intermediate for the formation of other anhydrosugars. Dehydration of levoglucosan and subsequent rearrangement may lead to the formation of 1,4:3,6-dianhydro-α-D-glucopyranose, 2,3-anhydro-D-mannosan, and 3,4-anhydro-D-galactosan.[1,15,49,50] Alternatively, dehydration at early stages disordered the cellulose structure, which made the residual sample inclined to the formation of other anhydrosugars other than LG during subsequent pyrolysis.

For the most part, the contents of hydrocarbons and aromatics increased with temperature. This is due to the increase in vapor cracking reactions with increasing temperature, which enhances reactions such as dehydrogenation, dehydration, decarbonylation, decarboxylation, and ring scission.[51−55] For instance, methyl alcohol (21.26% of stage 300 °C products) can undergo decomposition as temperature increases to form H_2, CH_2O, and CO. With further temperature increase, CO_2 and CH_4 can generate from the oxidation−reduction reaction between two CH_2O molecules.[52]

Generally, phenols increased with increasing temperature as more lignin decomposed at higher temperatures.[1,28] At 350 and 400 °C, the phenols detected were phenol, guaiacol, and its derivatives such as creosol, eugenol, and 2-methoxy-4-vinylphenol. At 450 °C, methyl phenols (i.e., cresols and xylenols such as 2-methyl phenol and 2,3-dimethyl phenol), hydroquinone, and derivatives of guaiacol were formed. As the temperature was further increased, more ethylphenols, methylphenols, and hydroquinones were formed, while the derivatives of guaiacol were reduced. At 500 °C, the selectivity of creosol was 21.62% and increased to 24.16% when the influence of noncondensing gases was removed. At 600 °C, the phenolic group produced was phenol and methyl phenols such as *o*-cresol, *m*-cresol, *o*-xylenol, 2,4-xylenol, and 3,4-xylenol. Guaiacols are the main product of lignin decomposition.[49] Hydrodeoxygenation (i.e., trans-alkylation, hydrogenation, hydrogenolysis, and deoxygenation, which includes dehydration, decarbonylation, and decarboxylation) of guaiacols can result in the formation of ethylphenols, methylphenols, and hydroquinones as temperature increases.[56]

In addition, aromatic ethers such as 2,3-dihydrobenzofuran can break down at higher temperatures to form phenols and radical fragments that can easily react with other volatiles to form other compounds.[55] Ketones and aldehydes were mainly formed from volatiles derived from single sugar ring breakdown.[12,28] In addition, ketonic decarboxylation (i.e., ketone formation from carboxylic acids) is likely to have occurred, leading to the reduction of the acid content. Since more nonsymmetrical ketones were produced, it suggests that the rate of cross-ketonization is faster than the rate of homoketonization. Nevertheless, due to dehydration at early stages, it was more favorable for ketones to be produced directly from depolymerization at the expense of carboxylic acids, which usually act as intermediates for ketone production.[57,58] The ketone content increased from 0 to 20.2% (300−450 °C) and then decreased to 0% at 600 °C. For

https://doi.org/10.1021/acsomega.1c05907
ACS Omega 2022, 7, 4245−4256

aldehydes, its contents generally decreased in the bio-oil with increasing temperature. Ring opening of intermediate monomers and cyclization might result in the production of cyclic ketones, ethers, alcohols, and aldehydes such as furfural and cyclohexanone, while fragmentation may lead to the production of lighter compounds such as acetone and formic acid.[59] The high yield of hydrocarbons and aromatics in the later stages can also be ascribed to the decrease of the oxygen content (i.e., the enrichment of acids, alcohols, and aldehydes in the early stages of pyrolysis) and the apparent increase of the lignin content in the remaining sample.[1,4,60] Furthermore, at later stages above 450 °C when conditions are more severe, the primary products formed can be readily converted into hydrocarbons through some condensation and isomerization reactions.[57]

Figure 9b shows the product distribution of various stages by the area. A temperature of 450 °C had the highest peak area, an affirmation of the DTG data, which suggests that maximum decomposition of the pine waste occurs between 400 and 450 °C. In general, it can be said that the peak area increased with increasing temperature until 450 °C, where decomposition was maximized. At 500 °C, the peak area reduced to about 2/7th of the peak area of 450 °C and continued to decrease in the later stages as temperature increased. The reduction of the peak area after 450 °C may suggest that (i) the majority of the biomass components, especially cellulose and hemicellulose, had been pyrolyzed in the earlier stages, making less and less of the biomass components available for further pyrolysis even at higher temperatures. (ii) The primary reaction of charring was maximized at 450 °C and continued at later stages, making it more difficult to break down the bonds holding the residual components of the biomass together. This corroborates why there is a sharp increase in the E_a value after the conversion of 0.75, as shown in graph (d) of Figures 3 and 4. The list of all compounds identified at each stage can be seen in the Supporting Information.

3.4.2. Direct Fast Pyrolysis. The acid content decreased with increasing temperature, thus corroborating the observation made by Cai et al.[1] that low-temperature pyrolysis of hemicellulose and cellulose produces acids and sugars. Zhang and his co-workers[16] also made a similar observation that the acid content of bio-oil decreases with increasing temperature. The phenol content decreased, while the aromatics increased as the temperature increased. This can be attributed to the thermal decomposition of reducing end groups and the dehydration reaction, as stated earlier.[17] For example, at 500 and 550 °C, only two aromatic compounds appeared (styrene and benzene, 4-ethenyl-1,2-dimethyl−), whereas, at an elevated temperature of 600 °C, simple aromatics like benzene, toluene, and xylene appeared as the end group of phenols either decomposed thermally or were dehydrated.

The aldehyde content increased with increasing temperature. Since phenols tend to react with aldehydes, it can be explained that as the temperature increased, it favored the reaction between phenols and aldehydes, which consequently contributed to the reduction of the phenol content as temperature increased.[1] At 500 °C, the selectivity of creosol was 7.81% and increased to 8.71% when the influence of noncondensing gases was removed. The aldehydes produced were mainly linear and branched aldehydes such as glyoxal, methyl glyoxal, 2-butenal, (E), nonanal, etc. The percentage of cyclic aldehydes produced decreased with an increase of temperature from 24.1% (500 °C) to 19.4% (600 °C). The content of alcohols and sugars slightly decreased before increasing marginally as temperature increased. Figure 10 shows the product distribution of the direct pyrolysis process.

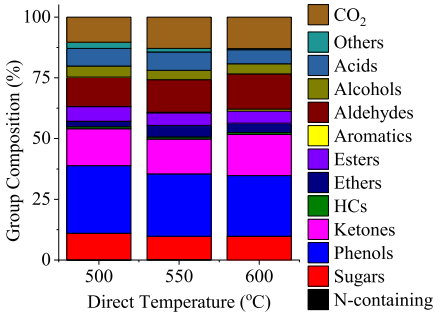

Figure 10. Product distribution of direct pyrolysis by the percentage.

3.4.3. Comparison of Staged and Direct Fast Pyrolysis. The staged pyrolysis process involved the pyrolysis of one sample at 300 °C and the subsequent pyrolysis of the residual sample from 350 to 600 °C at an interval of 50 °C per stage, while the direct pyrolysis involved the pyrolysis of a sample once at set temperatures of 500, 550, and 600 °C. To compare the functional group distribution of the staged pyrolysis process to that of the direct pyrolysis process, a cumulative group composition of the staged pyrolysis process was calculated at 500, 550, and 600 °C. The product distribution for direct pyrolysis and the cumulative product yield of staged pyrolysis can be seen in Figure 11. The acid, alcohol, aldehyde,

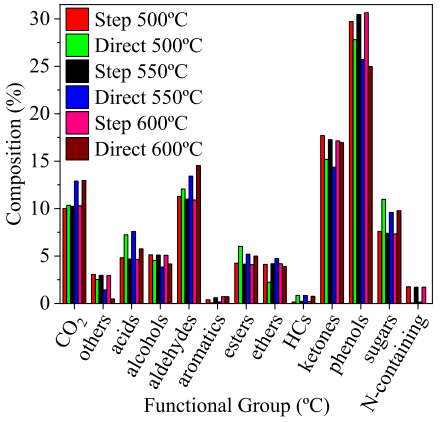

Figure 11. Product distribution of staged pyrolysis and direct pyrolysis.

ester, ketone, and sugar content of the bio-oil, all decreased slightly with an increase in the temperature for staged pyrolysis. However, for the direct pyrolysis, the acid and ether content first increased slightly before decreasing, while alcohols and ketones, on the other hand, decreased slightly first before increasing for direct pyrolysis. Nonetheless, the cumulative yield of acids was significantly lower for staged pyrolysis, while the ketones were much higher than direct pyrolysis. This suggests that ketonic decarboxylation of carboxylic acids was more profound in staged pyrolysis than in direct pyrolysis. However, at 600 °C, for direct pyrolysis, the acids reduced by about 2%, while the ketones correspondingly increased by that much, implying that severe conditions during direct pyrolysis favor ketonization. In the presence of water,

https://doi.org/10.1021/acsomega.1c05907
ACS Omega 2022, 7, 4245−4256

hydrolysis to form acids followed by ketonization of the acids is the preferred route for conversion of esters. The ester content for staged pyrolysis only decreased slightly, while that of direct pyrolysis decreased to a greater extent. This stems from the fact that dehydration occurs at early stages, making the water evolved less available for hydrolysis of the esters. On the other hand, water generated was readily available for ester hydrolysis in direct pyrolysis, hence the significant reduction.[57,58] For both types of pyrolysis, CO_2 slightly increased with an increase in temperature because high temperatures favor hydrodeoxygenation reactions, and CO_2 removal is a desirable route because it has the highest deoxygenation efficiency.[3] In both cases of pyrolysis, the aromatic content increased slightly with an increase in temperature.

The phenol content for staged pyrolysis increased with temperature, while it decreased for direct pyrolysis. This implies that during the staged pyrolysis process, more lignin was broken down, resulting in the increase. For direct pyrolysis, the reduction in the phenolic content may be ascribed to the reaction of some of the phenols with other compounds or their deoxygenation to form aromatics. At 600 °C of staged pyrolysis, the phenolic group comprised of only phenol and methyl phenols in contrast to that of direct pyrolysis, which had a mixture of both light phenols and methoxy phenols such as guaiacol and its derivatives.

Both direct and staged pyrolysis had aldehydes such as acetaldehyde, glyoxal, furfural, succindialdehyde, etc. However, vanillin was produced in all of the direct pyrolysis processes. but was only detected at 400 and 450 °C of the staged pyrolysis process. Benzaldehyde, 4-(*t*-butyl) benzaldehyde, 2-methyl-oct-2-enedial, 2,3,4,5-tetramethyl-benzaldehyde, and glutaraldehyde were produced only at the stages of 350, 400, 450, 500, and 550 °C, respectively, but were not produced in the direct pyrolysis process. Furthermore, *β*-methyl-cinnamaldehyde was only produced at 500 and 600 °C of the staged pyrolysis. Even though the oxygenate contents for both staged and direct pyrolysis decreased with increasing temperature, the reduction in the direct process was to a greater extent (3.12%) than that of the staged pyrolysis (0.63%). The cumulative bio-oil yields for staged pyrolysis at 500, 550, and 600 °C were 2.5, 3.6, and 3.8 times higher than the corresponding bio-oil yield for direct pyrolysis.

4. CONCLUSIONS

The staged and direct fast pyrolysis behavior and kinetics of waste pine sawdust were investigated using high heating rate TG-FTIR and Py-GC/MS. The apparent activation energy for high heating rate pyrolysis was about 60.13 kJ/mol higher than that of low heating rate pyrolysis. In addition, the active pyrolysis stage for the high heating rate pyrolysis had a wider range in comparison to that of slow pyrolysis. The most important deoxygenation reaction is the formation of carbon dioxide. Both DTG curves and Py-GC/MS staged pyrolysis showed that the major decomposition stage of pine is at 450 °C, with phenols, ketones, aldehydes, and sugars as the main products. For both the direct pyrolysis and the cumulative product of staged pyrolysis, the total oxygenate content decreased with an increase in temperature. For staged pyrolysis, different stages show significantly different product distributions. The selectivity of acids and aldehydes reached the peak value at 350 °C, while ketones and sugars reached their peak value at 450 °C. The selectivity of phenols significantly increased to over 50% after 500 °C. The staged pyrolysis process can hopefully be applied to produce certain specific compounds from biomass. In the pyrolysis stage of 500 °C, the selectivity of creosol reached 21.62% (if the influence of noncondensing gas is excluded, the value is 24.16%), about 3 times higher than that of direct pyrolysis.

■ ASSOCIATED CONTENT

Supporting Information

The Supporting Information is available free of charge at https://pubs.acs.org/doi/10.1021/acsomega.1c05907.

TG and DTG thermograms for 4 experimental runs (Figure S1), kinetic analysis (Table S1, Table S2), and identified compounds for staged pyrolysis (Table S3) (PDF)

■ AUTHOR INFORMATION

Corresponding Authors

Jinhong Zhang − *State Key Laboratory of Heavy Oil Processing, College of Chemical Engineering, China University of Petroleum, Qingdao 266580, China; Shandong Engineering and Technology Research Center of High Carbon Energy Low Carbonization, China University of Petroleum, Qingdao 266580, China;* orcid.org/0000-0002-0212-0503; Email: zhangjh@upc.edu.cn

Yuanyu Tian − *State Key Laboratory of Heavy Oil Processing, College of Chemical Engineering, China University of Petroleum, Qingdao 266580, China; Shandong Engineering and Technology Research Center of High Carbon Energy Low Carbonization, China University of Petroleum, Qingdao 266580, China;* orcid.org/0000-0003-3326-7484; Email: tianyy1008@126.com

Authors

Daniel T. Sekyere − *State Key Laboratory of Heavy Oil Processing, College of Chemical Engineering, China University of Petroleum, Qingdao 266580, China; Shandong Engineering and Technology Research Center of High Carbon Energy Low Carbonization, China University of Petroleum, Qingdao 266580, China;* orcid.org/0000-0001-5211-3072

Noah Niwamanya − *State Key Laboratory of Heavy Oil Processing, College of Chemical Engineering, China University of Petroleum, Qingdao 266580, China; Shandong Engineering and Technology Research Center of High Carbon Energy Low Carbonization, China University of Petroleum, Qingdao 266580, China*

Yansheng Huang − *State Key Laboratory of Heavy Oil Processing, College of Chemical Engineering, China University of Petroleum, Qingdao 266580, China; Shandong Engineering and Technology Research Center of High Carbon Energy Low Carbonization, China University of Petroleum, Qingdao 266580, China*

Andrew Barigye − *State Key Laboratory of Heavy Oil Processing, College of Chemical Engineering, China University of Petroleum, Qingdao 266580, China; Shandong Engineering and Technology Research Center of High Carbon Energy Low Carbonization, China University of Petroleum, Qingdao 266580, China*

Complete contact information is available at: https://pubs.acs.org/10.1021/acsomega.1c05907

Notes

The authors declare no competing financial interest.

■ ACKNOWLEDGMENTS

The authors acknowledge the financial support provided by the National Natural Science Foundation of China (22078363 and 21706287), the Fundamental Research Funds for the Central Universities (20CX02208A), and the Development Fund of State Key Laboratory of Heavy Oil Processing.

■ REFERENCES

(1) Cai, W.; Liu, Q.; Shen, D.; Wang, J. Py-GC/MS analysis on product distribution of two-staged biomass pyrolysis. *J. Anal. Appl. Pyrolysis* **2019**, *138*, 62−69.
(2) Muley, P. D.; Henkel, C.; Abdollahi, K. K.; Boldor, D. Pyrolysis and Catalytic Upgrading of Pinewood Sawdust Using an Induction Heating Reactor. *Energy Fuels* **2015**, *29*, 7375−7385.
(3) Wang, S.; Dai, G.; Yang, H.; Luo, Z. Lignocellulosic biomass pyrolysis mechanism: A state-of-the-art review. *Prog. Energy Combust. Sci.* **2017**, *62*, 33−86.
(4) Zhang, L.; Li, S.; Li, K.; Zhu, X. Two-step pyrolysis of corncob for value-added chemicals and high quality bio-oil: Effects of pyrolysis temperature and residence time. *Energy Convers. Manage.* **2018**, *166*, 260−267.
(5) Abnisa, F.; Wan Daud, W. M. A. A review on co-pyrolysis of biomass: An optional technique to obtain a high-grade pyrolysis oil. *Energy Convers. Manage.* **2014**, *87*, 71−85.
(6) Abnisa, F.; Wan Daud, W. M. A.; Ramalingam, S.; Azemi, M. N. B. M.; Sahu, J. N. Co-pyrolysis of palm shell and polystyrene waste mixtures to synthesis liquid fuel. *Fuel* **2013**, *108*, 311−318.
(7) Chen, H.; Xie, Y.; Chen, W.; Xia, M.; Li, K.; Chen, Z.; Chen, Y.; Yang, H. Investigation on co-pyrolysis of lignocellulosic biomass and amino acids using TG-FTIR and Py-GC/MS. *Energy Convers. Manage.* **2019**, *196*, 320−329.
(8) Kan, T.; Strezov, V.; Evans, T.; He, J.; Kumar, R.; Lu, Q. Catalytic pyrolysis of lignocellulosic biomass: A review of variations in process factors and system structure. *Renewable Sustainable Energy Rev.* **2020**, *134*, No. 110305.
(9) Miandad, R.; Barakat, M. A.; Aburiazaiza, A. S.; Rehan, M.; Nizami, A. S. Catalytic pyrolysis of plastic waste: A review. *Process Saf. Environ. Prot.* **2016**, *102*, 822−838.
(10) Zhang, X.; Lei, H.; Chen, S.; Wu, J. Catalytic co-pyrolysis of lignocellulosic biomass with polymers: a critical review. *Green Chem.* **2016**, *18*, 4145−4169.
(11) Cai, H.; Liu, J.; Xie, W.; Kuo, J.; Buyukada, M.; Evrendilek, F. Pyrolytic kinetics, reaction mechanisms and products of waste tea via TG-FTIR and Py-GC/MS. *Energy Convers. Manage.* **2019**, *184*, 436−447.
(12) Gao, N.; Li, A.; Quan, C.; Du, L.; Duan, Y. TG−FTIR and Py−GC/MS analysis on pyrolysis and combustion of pine sawdust. *J. Anal. Appl. Pyrolysis* **2013**, *100*, 26−32.
(13) Lu, X.; Zhu, X.; Guo, H.; Que, H.; Wang, D.; Liang, D.; He, T.; Hu, C.; Xu, C.; Gu, X. Investigation on the thermal degradation behavior of enzymatic hydrolysis lignin with or without steam explosion treatment characterized by TG-FTIR and Py-GC/MS. *Biomass Convers. Biorefin.* **2020**, DOI: 10.1007/s13399-020-00987-5.
(14) Zhang, J.; Liu, J.; Evrendilek, F.; Zhang, X.; Buyukada, M. TG-FTIR and Py-GC/MS analyses of pyrolysis behaviors and products of cattle manure in CO2 and N2 atmospheres: Kinetic, thermodynamic, and machine-learning models. *Energy Convers. Manage.* **2019**, *195*, 346−359.
(15) Westerhof, R. J. M.; Brilman, D. W. F.; Garcia-Perez, M.; Wang, Z.; Oudenhoven, S. R. G.; Kersten, S. R. A. Stepwise Fast Pyrolysis of Pine Wood. *Energy Fuels* **2012**, *26*, 7263−7273.
(16) Zhang, H.; Shao, S.; Jiang, Y.; Vitidsant, T.; Reubroycharoen, P.; Xiao, R. Improving hydrocarbon yield by two-step pyrolysis of pinewood in a fluidized-bed reactor. *Fuel Process. Technol.* **2017**, *159*, 19−26.
(17) Zhang, L.; Li, S.; Huang, L.; Zhu, X. Two-step pyrolysis characteristic of cellulose: effects of pyrolysis temperature and residence time. *Energy Sources, Part A* **2019**, *41*, 2481−2493.
(18) Trubetskaya, A.; Attard, T. M.; Budarin, V. L.; Hunt, A. J.; Arshadi, M.; Grams, J. Supercritical Extraction of Biomass—A Green and Sustainable Method to Control the Pyrolysis Product Distribution. *ACS Sustainable Chem. Eng.* **2021**, *9*, 5278−5287.
(19) Arenas, C. N.; Navarro, M. V.; Martinez, J. D. Pyrolysis kinetics of biomass wastes using isoconversional methods and the distributed activation energy model. *Bioresour. Technol.* **2019**, *288*, No. 121485.
(20) Ong, H. C.; Chen, W.-H.; Singh, Y.; Gan, Y. Y.; Chen, C.-Y.; Show, P. L. A state-of-the-art review on thermochemical conversion of biomass for biofuel production: A TG-FTIR approach. *Energy Convers. Manage.* **2020**, *209*, No. 112634.
(21) White, J. E.; Catallo, W. J.; Legendre, B. L. Biomass pyrolysis kinetics: A comparative critical review with relevant agricultural residue case studies. *J. Anal. Appl. Pyrolysis* **2011**, *91*, 1−33.
(22) Wu, K.; Liu, J.; Wu, Y.; Chen, Y.; Li, Q.; Xiao, X.; Yang, M. Pyrolysis characteristics and kinetics of aquatic biomass using thermogravimetric analyzer. *Bioresour. Technol.* **2014**, *163*, 18−25.
(23) Hao, J.; Che, Y.; Tian, Y.; Li, D.; Zhang, J.; Qiao, Y. Thermal Cracking Characteristics and Kinetics of Oil Sand Bitumen and Its SARA Fractions by TG−FTIR. *Energy Fuels* **2017**, *31*, 1295−1309.
(24) Qiao, Y.; Xu, F.; Xu, S.; Yang, D.; Wang, B.; Ming, X.; Hao, J.; Tian, Y. Pyrolysis Characteristics and Kinetics of Typical Municipal Solid Waste Components and Their Mixture: Analytical TG-FTIR Study. *Energy Fuels* **2018**, *32*, 10801−10812.
(25) Wang, B.; Xu, F.; Zong, P.; Zhang, J.; Tian, Y.; Qiao, Y. Effects of heating rate on fast pyrolysis behavior and product distribution of Jerusalem artichoke stalk by using TG-FTIR and Py-GC/MS. *Renewable Energy* **2019**, *132*, 486−496.
(26) Mishra, G.; Kumar, J.; Bhaskar, T. Kinetic studies on the pyrolysis of pinewood. *Bioresour. Technol.* **2015**, *182*, 282−288.
(27) Shi, X.; Wang, J. A comparative investigation into the formation behaviors of char, liquids and gases during pyrolysis of pinewood and lignocellulosic components. *Bioresour. Technol.* **2014**, *170*, 262−269.
(28) Wang, J.-X.; Cao, J.-P.; Zhao, X.-Y.; Liu, T.-L.; Wei, F.; Fan, X.; Zhao, Y.-P.; Wei, X.-Y. Study on pine sawdust pyrolysis behavior by fast pyrolysis under inert and reductive atmospheres. *J. Anal. Appl. Pyrolysis* **2017**, *125*, 279−288.
(29) Maia, A. A. D.; de Morais, L. C. Kinetic parameters of red pepper waste as biomass to solid biofuel. *Bioresour. Technol.* **2016**, *204*, 157−163.
(30) Mehmood, M. A.; Ahmad, M. S.; Liu, Q.; Liu, C.-G.; Tahir, M. H.; Aloqbi, A. A.; Tarbiah, N. I.; Alsufiani, H. M.; Gull, M. Helianthus tuberosus as a promising feedstock for bioenergy and chemicals appraised through pyrolysis, kinetics, and TG-FTIR-MS based study. *Energy Convers. Manage.* **2019**, *194*, 37−45.
(31) Navarro, M. V.; López, J. M.; Veses, A.; Callén, M. S.; García, T. Kinetic study for the co-pyrolysis of lignocellulosic biomass and plastics using the distributed activation energy model. *Energy* **2018**, *165*, 731−742.
(32) Slopiecka, K.; Bartocci, P.; Fantozzi, F. Thermogravimetric analysis and kinetic study of poplar wood pyrolysis. *Appl. Energy* **2012**, *97*, 491−497.
(33) Alam, M.; Bhavanam, A.; Jana, A.; Viroja, J. kS.; Peela, N. R. Co-pyrolysis of bamboo sawdust and plastic: Synergistic effects and kinetics. *Renewable Energy* **2020**, *149*, 1133−1145.
(34) Stefanidis, S. D.; Kalogiannis, K. G.; Iliopoulou, E. F.; Michailof, C. M.; Pilavachi, P. A.; Lappas, A. A. A study of lignocellulosic biomass pyrolysis via the pyrolysis of cellulose, hemicellulose and lignin. *J. Anal. Appl. Pyrolysis* **2014**, *105*, 143−150.
(35) Xu, F.; Wang, B.; Yang, D.; Ming, X.; Jiang, Y.; Hao, J.; Qiao, Y.; Tian, Y. TG-FTIR and Py-GC/MS study on pyrolysis mechanism and products distribution of waste bicycle tire. *Energy Convers. Manage.* **2018**, *175*, 288−297.
(36) Hu, M.; Chen, Z.; Guo, D.; Liu, C.; Xiao, B.; Hu, Z.; Liu, S. Thermogravimetric study on pyrolysis kinetics of Chlorella

https://doi.org/10.1021/acsomega.1c05907
ACS Omega 2022, 7, 4245−4256

pyrenoidosa and bloom-forming cyanobacteria. *Bioresour. Technol.* **2015**, *177*, 41−50.
(37) Burhenne, L.; Messmer, J.; Aicher, T.; Laborie, M.-P. The effect of the biomass components lignin, cellulose and hemicellulose on TGA and fixed bed pyrolysis. *J. Anal. Appl. Pyrolysis* **2013**, *101*, 177−184.
(38) Li, J.; Qiao, Y.; Zong, P.; Qin, S.; Wang, C.; Tian, Y. Fast pyrolysis characteristics of two typical coastal zone biomass fuels by thermal gravimetric analyzer and down tube reactor. *Bioresour. Technol.* **2019**, *283*, 96−105.
(39) Wani Likun, P. K.; Zhang, H. Insights into pyrolysis of torrefied-biomass, plastics/tire and blends: Thermochemical behaviors, kinetics and evolved gas analyses. *Biomass Bioenergy* **2020**, *143*, No. 105852.
(40) Yang, H.; Yan, R.; Chen, H.; Lee, D. H.; Zheng, C. Characteristics of hemicellulose, cellulose and lignin pyrolysis. *Fuel* **2007**, *86*, 1781−1788.
(41) Yu, J.; Paterson, N.; Blamey, J.; Millan, M. Cellulose, xylan and lignin interactions during pyrolysis of lignocellulosic biomass. *Fuel* **2017**, *191*, 140−149.
(42) Liu, Q.; Zhong, Z.; Wang, S.; Luo, Z. Interactions of biomass components during pyrolysis: A TG-FTIR study. *J. Anal. Appl. Pyrolysis* **2011**, *90*, 213−218.
(43) Shi, L.; Yu, S.; Wang, F.-C.; Wang, J. Pyrolytic characteristics of rice straw and its constituents catalyzed by internal alkali and alkali earth metals. *Fuel* **2012**, *96*, 586−594.
(44) Wang, S.; Wang, K.; Liu, Q.; Gu, Y.; Luo, Z.; Cen, K.; Fransson, T. Comparison of the pyrolysis behavior of lignins from different tree species. *Biotechnol. Adv.* **2009**, *27*, 562−567.
(45) Wang, S.; Guo, X.; Liang, T.; Zhou, Y.; Luo, Z. Mechanism research on cellulose pyrolysis by Py-GC/MS and subsequent density functional theory studies. *Bioresour. Technol.* **2012**, *104*, 722−728.
(46) Liu, D.; Yu, Y.; Hayashi, J.-i.; Moghtaderi, B.; Wu, H. Contribution of dehydration and depolymerization reactions during the fast pyrolysis of various salt-loaded celluloses at low temperatures. *Fuel* **2014**, *136*, 62−68.
(47) Wang, X.; Zhu, S.; Wang, S.; He, Y.; Liu, Y.; Wang, J.; Fan, W.; Lv, Y. Low temperature hydrodeoxygenation of guaiacol into cyclohexane over Ni/SiO2 catalyst combined with Hβ zeolite. *RSC Adv.* **2019**, *9*, 3868−3876.
(48) Lu, Q.; Wu, Y.-t.; Hu, B.; Liu, J.; Liu, D.-j.; Dong, C.-q.; Yang, Y.-p. Insight into the mechanism of secondary reactions in cellulose pyrolysis: interactions between levoglucosan and acetic acid. *Cellulose* **2019**, *26*, 8279−8290.
(49) Ahmad, E.; Pant, K. K. Lignin Conversion: A Key to the Concept of Lignocellulosic Biomass-Based Integrated Biorefinery. *Waste Biorefin.* **2018**, 409−444.
(50) Kim, J.-S.; Choi, G.-G. Pyrolysis of Lignocellulosic Biomass for Biochemical Production. *Waste Biorefin.* **2018**, 323−348.
(51) Moldoveanu, S. C. Pyrolysis of Carboxylic Acids. In *Pyrolysis of Organic Molecules: Applications to Health and Environmental Issues*; 2nd ed.; Elsevier B.V., 2019; Vol. 2, pp 483−553.
(52) Moldoveanu, S. C. Pyrolysis of Alcohols and Phenols. In *Pyrolysis of Organic Molecules: Applications to Health and Environmental Issues*; 2nd ed.; Elsevier B.V., 2019; Vol. 2, pp 207−278.
(53) Moldoveanu, S. C. Pyrolysis of Aldehydes and Ketones. In *Pyrolysis of Organic Molecules: Applications to Health and Environmental Issues*; 2nd ed.; Elsevier B.V, 2019; Vol. 2, pp 391−418.
(54) Moldoveanu, S. C. Pyrolysis of Hydrocarbons. In *Pyrolysis of Organic Molecules: Applications to Health and Environmental Issues*; 2nd ed.; Elsevier B.V., 2019; pp 35−161.
(55) Moldoveanu, S. C. Pyrolysis of Ethers. *Pyrolysis of Organic Molecules* **2019**, 279−310.
(56) He, Y.; Bie, Y.; Lehtonen, J.; Liu, R.; Cai, J. Hydrodeoxygenation of guaiacol as a model compound of lignin-derived pyrolysis bio-oil over zirconia-supported Rh catalyst: Process optimization and reaction kinetics. *Fuel* **2019**, *239*, 1015−1027.
(57) Renz, M. Ketonization of Carboxylic Acids by Decarboxylation: Mechanism and Scope. *Eur. J. Org. Chem.* **2005**, *2005*, 979−988.
(58) Gaertner, Christian A.; S-R, J. C.; Braden, Drew J.; Dumesic, James A. Ketonization Reactions of Carboxylic Acids and Esters over Ceria-Zirconia as Biomass Upgrading Process. *Ind. Eng. Chem. Res.* **2010**, *49*, 6027−6033.
(59) Hu, X.; Gholizadeh, M. Biomass pyrolysis: A review of the process development and challenges from initial researches up to the commercialisation stage. *J. Energy Chem.* **2019**, *39*, 109−143.
(60) Hammer, N. L.; Garrido, R. A.; Starcevich, J.; Coe, C. G.; Satrio, J. A. Two-Step Pyrolysis Process for Producing High Quality Bio-oils. *Ind. Eng. Chem. Res.* **2015**, *54*, 10629−10637.

https://doi.org/10.1021/acsomega.1c05907
ACS Omega 2022, 7, 4245−4256